Adsorption (2011) 17: 303–309
DOI 10.1007/s10450-010-9287-1

Neural network modelling of adsorption isotherms

Graham Morse · Rudy Jones · Jules Thibault · F. Handan Tezel

Received: 19 March 2008 / Accepted: 20 October 2010 / Published online: 4 November 2010

Abstract This paper examines the possibility to use a single neural network to model and predict a wide array of standard adsorption isotherm behaviour. Series of isotherm data were generated from the four most common isotherm equations (Langmuir, Freundlich, Sips and Toth) and the data were fitted with a unique neural network structure. Results showed that a single neural network with a hidden layer having three neurons, including the bias neuron, was able to represent very accurately the adsorption isotherm data in all cases. Similarly, a neural network with four hidden neurons, including the bias, was able to predict very accurately the temperature dependency of adsorption data.

Keywords Isotherms · Neural networks · Langmuir · Freundlich · Sips · Toth

Nomenclature

A	constant for Freundlich equation (kg ethanol/kg adsorbent) $(m^3/kg\ ethanol)^{1/n}$
b	constant for Langmuir, Toth and Sips equations; temperature dependent variable for the TD-Toth equation (m^3/kg adsorbate)
b_o	constant for the TD-Toth equation (m^3/kg adsorbate)
c	fluid adsorbate concentration (kg adsorbate/m^3)
n	constant for the Freundlich and Sips equations (dimensionless)
q	solid adsorbate concentration (kg adsorbate/kg solids)
q_s	saturation capacity—constant for Langmuir, Sips, Toth equations; temperature dependent variable for the TD-Toth equation (kg adsorbate/kg solids)
q_{so}	constant for the TD-Toth equation (kg adsorbate/kg solids)
Q	heat of adsorption (J/mol adsorbed)
R	gas constant (8.314 Pa m^3/(mol K) or 8.314 J/(mol K))
t	temperature dependent variable for TD-Toth equation (dimensionless)
t_o	constant for the TD-Toth equation (dimensionless)
T	temperature (°C or K)
T_o	reference temperature (°C or K)
W	neural network weights between the input and hidden layers parameters of (6)
W'	neural network weights between the hidden and output layers

Greek symbols

α	constant for the TD-Toth equation (dimensionless)
χ	constant for the TD-Toth equation (dimensionless)

Upperscript

–	normalized values

Subscripts

i	neuron number in input layer
j	neuron number in hidden layer
k	neuron number in output layer

G. Morse · R. Jones · J. Thibault (✉) · F.H. Tezel
Department of Chemical Engineering, University of Ottawa, Ottawa, ON, Canada K1N 6N5
e-mail: Jules.Thibault@uottawa.ca

Abbreviations

ANN	Artificial Neural networks
BDDT	Brunauer, Deming, Deming and Teller
FFNN	Feed-forward neural networks
IUPAC	International Union of Pure and Applied Chemistry
TD	Temperature Dependent

1 Introduction

Adsorption is a commonly used chemical engineering separation process. It is a process whereby two or more components of a fluid (gas or liquid) stream are separated through contact with a solid surface. The quantity of the component which can bind to the surface of the adsorbent will depend on the temperature and the composition (partial pressure or concentration) as well as various physical and chemical properties of the adsorbate-adsorbent pair. A measurement of the amount adsorbed over a range of compositions at a fixed temperature is known as an adsorption isotherm.

It is difficult to predict a priori the isotherm behaviour of a particular system because of the inherent complexities associated with adsorption. The differing properties of fluids and solids are the key variables affecting this equilibrium. A given fluid or solid can be formed with an infinite variety of differing compositions and components. This creates a myriad of possibilities and scenarios when attempting to model the interactions.

The majority of experimental isotherm data observed can be classified into six defined "types". Brunauer, Deming, Deming and Teller (BDDT) classification in 1940 recognized five distinct isotherm trends (Brunauer et al. 1940), and in 1985 the International Union of Pure and Applied Chemistry (IUPAC) introduced a sixth general isotherm trend which makes up the accepted isotherm classification system (Sing et al. 1985).

Over the years, many adsorption isotherm systems have been modeled using particular equations. These include Langmuir, Freundlich, Sips, and Toth isotherm models among others. Although these classic adsorption isotherm models are capable of representing certain equilibrium data sets by themselves, they also display a considerable lack of fit when modelling non-traditional systems. The variable nature of these adsorption isotherms presents a challenge to the development of an equation that can be used to model the behaviour of all adsorption systems. For example, Padmesh et al. (2006) used a total of ten different isotherm correlations in an attempt to find a suitable equation that will fit their adsorption data. To date, a single unifying equation to model all types of adsorption isotherms has yet to be constructed.

A general adsorption model must successfully address the following criteria. It must be: (1) flexible enough to deal with the wide variety of isotherms; (2) able to predict the trends between any two data points; (3) fit the visual trends of the data set; and (4) able to include known trends that are characteristic of adsorption.

Because the driving force for all adsorption separations will depend on the existence of a departure from equilibrium, it is imperative that an accurate and versatile adsorption isotherm model for a system is attained before design, simulation or modelling can be accomplished. Artificial neural networks are a general class of nonlinear models that have the potential to address the above criteria.

The scope of this paper is therefore to examine if a single artificial neural network structure can be used as a comprehensive adsorption model. In other words, it is desired to find a suitable model to represent adsorption data where only the parameters of the fixed-structure model will change such that one will not have to search for the most appropriate structure of the model (Langmuir, Freundlich, Sips, Toth…) as it is currently being done in practice. Feed-forward neural networks have been successfully used in many applications related to adsorption. It was used to simulate the dynamics of an adsorption column for wastewater treatment of water containing toxic chemicals (Bulsari and Palosaafi 1993) and to predict the occurrence of breakthrough in an ion-exchange adsorption column (Yang et al. 1993). Lewandowski et al. (1998) developed a method for the simulation and optimization of a pressure swing adsorption process for the separation of nitrogen from air where the neural network model was used to obtain a prediction for the process performance, namely, the specific product and yield, over a wide range of operating conditions. Carsky and Do (1999) predicted the adsorption equilibrium of binary vapour mixtures on activated carbon. Sundaram (1999) used a neural network to analyze the relationship between input and output variables for pressure swing adsorption (PSA) processes for three different applications. Basu et al. (2002) predicted the effect of temperature on equilibrium adsorption of hydrocarbon gases and vapours on activated carbon. Basu et al. (2002) used a neural network to predict the pollutant removal efficiency based on a large data bank of pollutants and adsorbents whereas neural networks were used by Gao and Engell (2004) to predict the slope, instead of the actual value, of nonlinear isotherms. Mjalli et al. (2005) used neural networks to represent the adsorption data for isopropanol-water system. Giraudet et al. (2006) predicted with a neural network the heat of adsorption from physical characteristics of activated carbons and volatile organic compound molecular properties. Vasina et al. (2009) used neural networks to model protein adsorption. Kumar et al. (2010) used a three-layer feed-forward artificial neural network to model the equilibrium data of hydrogen onto activated carbons. The properties of the activated carbons and the experimental conditions were used as inputs to predict

Table 1 Modelling results obtained with the four types of isotherms

Isotherm	Equation	Set	Parameters	$\sum(q-\hat{q})^2$
Langmuir	$q=\frac{q_s bc}{1+bc}$	1	$(q_s, b)=(1, 7)$	8.55×10^{-6}
		2	$(1, 100)$	1.51×10^{-3}
		3	$(150, 0.00670)$	3.7×10^{-15}
Freundlich	$q=Ac^{1/n}$	1	$(A, n)=(1, 1)$	3.97×10^{-15}
		2	$(1, 0.1)$	9.86×10^{-7}
		3	$(1, 10)$	2.96×10^{-2}
		4	$(1, 0.3)$	3.70×10^{-8}
		5	$(1, 3)$	1.27×10^{-3}
Sips	$q=\frac{q_s(bc)^{1/n}}{1+(bc)^{1/n}}$	1	$(39.7, 0.273, 0.985)$	1.28×10^{-7}
(Langmuir-		2	$(q_s, b, t)=(1, 50, 1)$	3.34×10^{-19}
Freundlich)		3	$(1, 3, 0.2)$	1.49×10^{-3}
Toth	$q=\frac{q_s bc}{[1+(bc)^t]^{1/t}}$	1	$(3.088, 0.325, 3.60)$	1.18×10^{-10}
		2	$(q_s, b, t)=(1, 50, 1)$	3.34×10^{-18}
		3	$(1, 3, 3)$	7.22×10^{-4}
TD Toth	$q=\frac{q_s bc}{[1+(bc)^t]^{1/t}}$	40 °C	$b_o=5.685$	3.67×10^{-4}
		70 °C	$(Q/RT_o)=7.029$	3.27×10^{-4}
		80 °C	$T_o=313.15$	2.07×10^{-4}
		100 °C	$t_o=0.706;\ \alpha=0,$	2.36×10^{-4}
		140 °C	$q_{so}=1.475;\ \chi=0$	3.79×10^{-4}

the corresponding hydrogen uptake at equilibrium conditions.

In this paper, it is desired to extend the use of neural network as a universal isotherm model. This paper is divided into sections as follows: it starts with a brief presentation of the most common isotherms that will be used to evaluate the ability of artificial neural networks to represent a wide variety of isotherm data. It is followed by the description of the artificial neural network structure that will be used to obtain these isotherm models. In the subsequent section, results are presented and discussed. Finally, results for temperature-dependent isotherms are presented.

2 Common adsorption isotherms

Four of the most common isotherms are used in this investigation to generate different series of adsorption data that will serve as learning data sets to fit artificial neural networks. It is desired to test if a single neural network structure can be used to represent the data of all simulated isotherm data. The four types of isotherms are Langmuir, Freundlich, Sips (Langmuir-Freundlich) and Toth.

The first isotherm, the Langmuir isotherm (Langmuir 1918) applies to localized adsorption of monolayer surface coverage assuming that each adsorbed molecule occupies one adsorption site. The derivation of the Langmuir isotherm was obtained by considering both the rates of adsorption and desorption, integrating the net rate of surface coverage and, at equilibrium, the isotherm equation reduces to the simple two-parameter equation presented in Table 1. Another isotherm, the Freundlich isotherm (Freundlich 1907), is a semi-empirical equation which is widely used to represent adsorption equilibrium data for low to intermediate range of concentration. The Freundlich equation is characterized with two fitting parameters and is presented in Table 1. The Sips isotherm (Sips 1948) is a combination of the Langmuir and Freundlich isotherms, which represent systems for which one adsorbed molecule could occupy more than one adsorption site (represented by the variable n in the isotherm equation given in Table 1). It has three parameters that could be expressed as a function of temperature which allows easy interpolation and extrapolation of the experimental isotherms to other temperatures and compositions. Another isotherm that has three parameters that could be written as a function of temperature is the Temperature Dependent (TD) Toth isotherm (Toth 1971). The equation for that isotherm is also given in Table 1.

To account for temperature dependency, parameters of isotherm equations are correlated as a function of temperature. For instance, the three parameters (q_s, b, and t) for the TD Toth isotherm are expressed as a function of temper-

ature by (1)–(3).

$$b = b_o \exp\left[\frac{Q}{RT_o}\left(\frac{T_o}{T} - 1\right)\right] \tag{1}$$

$$t = t_o + \alpha\left(1 - \frac{T_o}{T}\right) \tag{2}$$

$$q_s = q_{so} \exp\left[\chi\left(1 - \frac{T}{T_o}\right)\right] \tag{3}$$

When these parameters are inserted into the regular Toth isotherm as a function of temperature, then the TD Toth isotherm (q as a function of c) becomes a correlation with a total of seven parameters: b_o, (Q/RT_o), T_o, t_o, α, q_{so}, and χ.

3 Neural network models

Neural networks have been the subject of considerable research interest for the past twenty years. Artificial neural networks (ANN) attempt to mimic how a biological system functions and how they can be utilized for their novel architecture to solve highly complex, undefined and nonlinear mathematical problems. ANNs can simply be viewed as general nonlinear models which have the ability to encapsulate the underlying relationship that exists between a series of inputs and outputs of a system. Hoskins and Himmelblau (1988) and Bhat and McAvoy (1989) appear to be the first authors that modelled chemical processes with an artificial neural network. Artificial neural networks are now being used for a wide variety of engineering applications. They possess a high degree of flexibility and plasticity that allows them to easily capture the nonlinear behaviour of a process using input-output data.

Feedforward neural networks (FFNN) are undoubtedly the most popular neural network structure used in engineering applications. It has been shown that a three-layer FFNN can represent any function provided that sufficient number of neurons are present (Cybenko 1989). A FFNN normally consists of three layers: an input layer, a hidden layer, and an output layer. The feedforward neural networks that have been used in this investigation are presented in Fig. 1. The input layer receives the process inputs and fans out this information to all functional neurons of the hidden layer. Each neuron of the hidden layer essentially performs two tasks: (1) a weighted summation of all process inputs; and (2) a non-linear transformation, via a neuron transfer function, of the weighted summation to produce the output of each neuron of the hidden layer which then serves as inputs to the neurons of the output layer. The output layer performs the same task as the neurons of the second layer to produce the final output of the FFNN. The typical transfer functions that are used in the hidden and output layers are linear, sigmoid

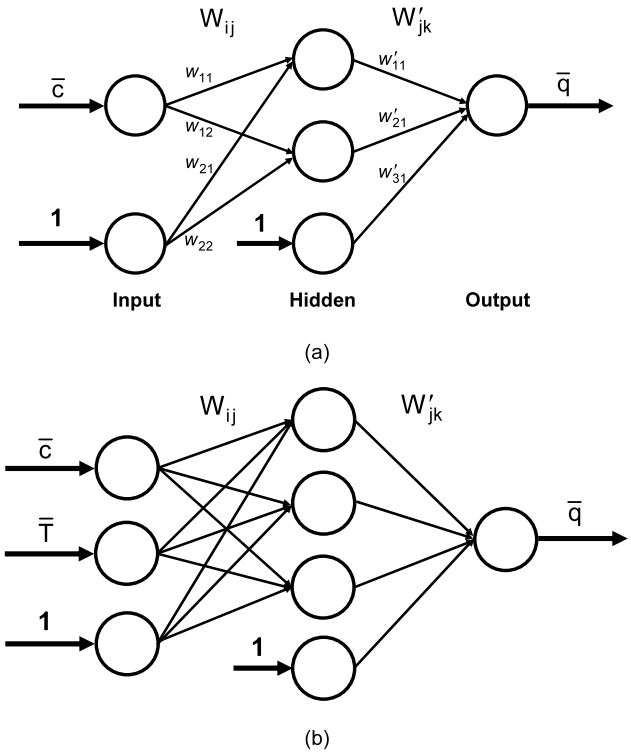

Fig. 1 Feedforward neural networks used to represent (**a**) all isotherm data sets at a given temperature, and (**b**) temperature-dependent isotherm data sets

or hyperbolic tangent. The input and output to the FFNN are usually scaled between 0 and 1 or −1 to 1. Results obtained with many neural network structures with different transfer functions were very similar such that it was decided to use a conventional structure with sigmoid transfer functions for the hidden layer and a linear transfer function for the output layer. Therefore, the resulting equation for the FFNN with three hidden neurons (including the bias) of Fig. 1(a) with scaled input and output is

$$\bar{q} = \frac{w'_{11}}{1 + e^{-(w_{11}\bar{c} + w_{21})}} + \frac{w'_{21}}{1 + e^{-(w_{12}\bar{c} + w_{22})}} + w'_{31} \tag{4}$$

$$\text{with } \bar{q} = \frac{q - q_{\min}}{q_{\max} - q_{\min}} \quad \text{and} \quad \bar{c} = \frac{c - c_{\min}}{c_{\max} - c_{\min}} \tag{5}$$

In a neural network, the fitting information lies in the interconnection weights or parameters (W_{ij} and W'_{jk} in Fig. 1) between neurons and the topology of the network. Using an ANN to represent experimental data between dependent and independent variables is no different than using any empirical model. The learning process consists of determining the weight matrices, W_{ij} and W'_{jk} that produce the best fit of the predicted outputs over the entire data set. In this investigation, the quasi-Newton optimization algorithm was used to fit the adsorption data (Powell 1975).

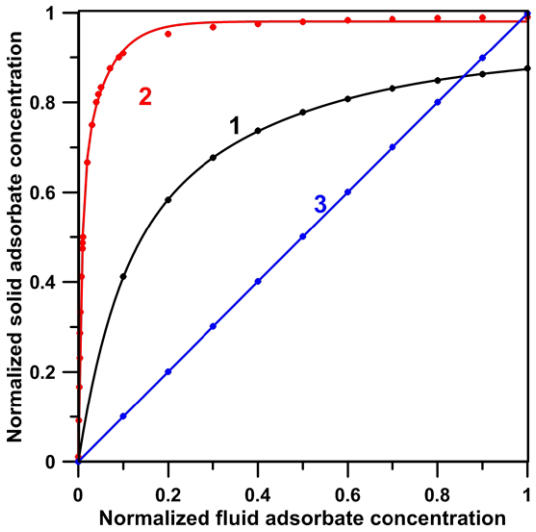

Fig. 2 FFNN for three Langmuir isotherm data sets. *Symbols* represent isotherm data and *curves* represent FFNN fits. The numbers refer to the models of Table 1

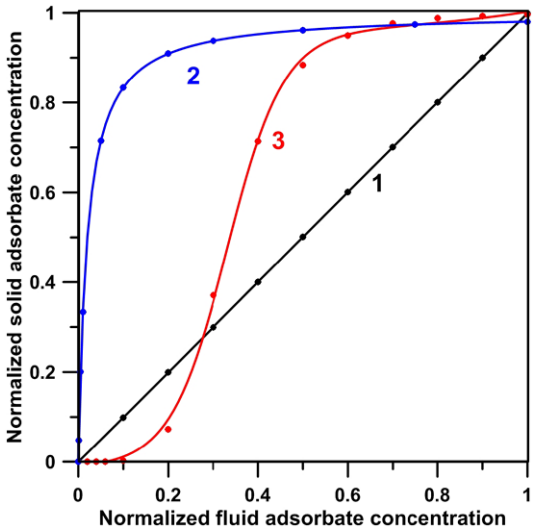

Fig. 4 FFNN for three SIPS isotherm data sets. *Symbols* represent isotherm data and *curves* represent FFNN fits. The numbers refer to the models of Table 1

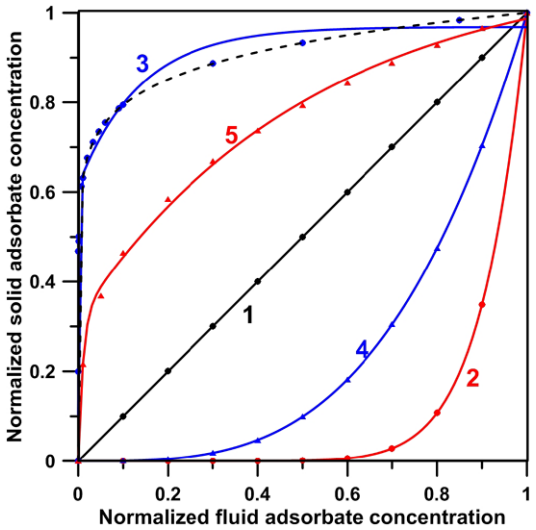

Fig. 3 FFNN for five Freundlich isotherm data sets. *Symbols* represent isotherm data and *curves* represent FFNN fits. The numbers refer to the models of Table 1

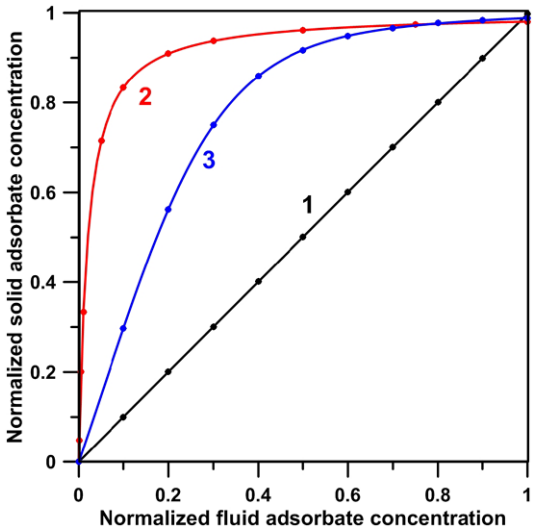

Fig. 5 FFNN for three Toth isotherm data sets. *Symbols* represent isotherm data and *curves* represent FFNN fits. The numbers refer to the models of Table 1

4 Results and discussion

4.1 Neural networks for modelling isotherms

The ultimate goal of this investigation was to test the ability of simple artificial neural network architectures with the least number of parameters to represent a wide variety of isotherm data. The four most commonly used temperature-independent two and three-parameter isotherms (see Table 1) were simulated over a wide range of parameter values and the generated data were fitted using the neural network architecture of Fig. 1(a) with three hidden neurons, including the bias. This neural network consists of one independent variable (the adsorbate fluid concentration, c) and one dependent variable (the adsorbate solids concentration, q). There are a total of seven neural network weights or model parameters.

Figures 2–5 present the results obtained for the four series of isotherm data. The data points in these figures were created by fixing the parameters of the isotherms differently for different data sets as given in Table 1. The FFNN in Fig. 1(a) was used to fit these data points. The sums of squares of the differences between the observed or simulated isotherm data and the fitted isotherm data for each set

are presented in the fifth column of Table 1. The solid lines on the graphs were obtained by predicting 100 equally distant predicted values in the range of the isotherm data points by using the fitted isotherm neural networks to ensure that the prediction was also good between observed data points that were used to fit the neural network. The 100 equally distributed points were also compared with the isotherm data that were generated from the models of Table 1 and similar prediction average errors were observed than for the points that were used for training the neural network. It is clear that the neural network of Fig. 1(a) is able to represent the large majority of isotherm data sets. The largest deviations are observed when the isotherm is strongly favourable. The most severe discrepancy was for the third set of the Freundlich isotherm data (Fig. 3). With only three hidden neurons (including the bias neuron), the simple neural network architecture of Fig. 1(a) was not sufficient to capture the strong nonlinearity that exists between the fluid and solid adsorbate concentrations. By adding a fourth hidden neuron for this particular isotherm data set, the fit was significantly improved as shown by the dotted line in Fig. 3. It was only under this extremely steep isotherm that it was necessary to use an additional neural to represent the adsorption data with a very precision. All the other isotherms were very well fitted with the neural network structure of Fig. 1(a) such that the predicted isotherm is of sufficient precision to be used with confidence for simulation and design.

The data of Padmesh et al. (2006) for the adsorption of acid red 88 from an aqueous solution at pH 3 by algal biomass was digitized so that it could be used to evaluate the performance of FFNN to fit adsorption data that deviate from a standard isotherm trend. Indeed, the experimental isotherm is extremely steep at low concentration in solution and has two distinct plateaus for which the most common isotherm equations listed in Table 1 are not able to represent adequately the experimental data by themselves. Figure 6 presents the results obtained with the FFNN with three and four hidden neurons, respectively. It is clear that the neural network of Fig. 1(a) was not able to perfectly capture the shape displayed by the experimental data. However, by adding another hidden neuron to the FFNN, the fit is excellent. The sums of squares of the errors were 10.5 and 0.012, respectively for the fit with three and four hidden neurons. This example shows clearly the enviable flexibility of neural network isotherm models over more conventional isotherm models.

4.2 Extension to include the temperature effect

In many adsorption applications, temperature effects are important and must be accounted for. It is important to have a reliable model that can fit a temperature-dependent adsorption isotherm over a given range of temperature. Artificial neural networks can be easily adapted to include the

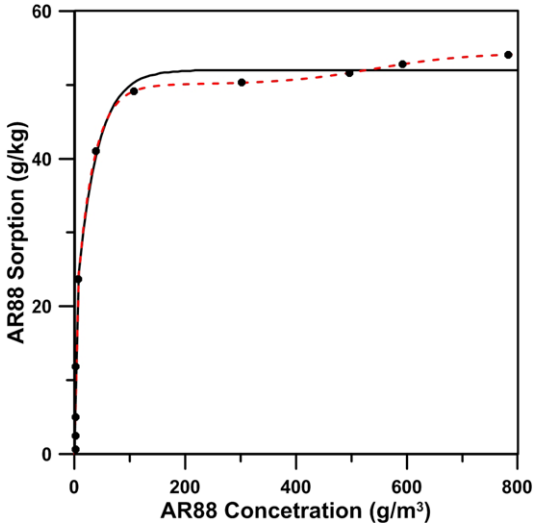

Fig. 6 FFNN for the data of Padmesh et al. (2006). *Symbols* represent experimental data and *curves* represent FFNN fits: *solid line*—FFNN with three hidden neurons; *dashed line*—FFNN with four hidden neurons

effect of temperature by adding an extra input neuron as well as adding one or more neurons in the hidden layer to take into consideration the additional complexity of the adsorption isotherm relationship. The temperature-dependent Toth adsorption isotherm model was used to generate series of isotherm data at five different temperatures, using the 7 parameters given in Table 1. Four of these series (40, 70, 100, and 140 °C) were used as the training data set to fit the temperature dependent neural network isotherm and the remaining series (80 °C) was used as the validation data set to assess the performance of the neural network predictions for the isotherm data that were not used during the fitting process. Results for these tests are presented in Fig. 7 and Table 1 for the neural network architecture of Fig. 1(b). The neural network model is able to predict very well the observed data points for both the training and validation data sets. In addition, to ensure that the model is a good representation of the isotherm data over the whole range of concentration and not only at the observed points, 100 equally distant values of the adsorbed concentration in the range of the isotherm data points were generated using the fitted isotherm neural networks. As can be observed, the generated curves (solid lines) are smooth and follow the trend that is expected from the isotherm data.

The accuracy of the fit is truly excellent. As a result, one could use the neural isotherm model with confidence in simulation and design. Here again, parsimony in the number of hidden neurons was targeted in order to have the simplest possible model. The neural network of Fig. 1(b) contains four hidden neurons. With five hidden neurons, slightly better predictions were obtained. When six hidden neurons were tested, better predictions were obtained for the learning

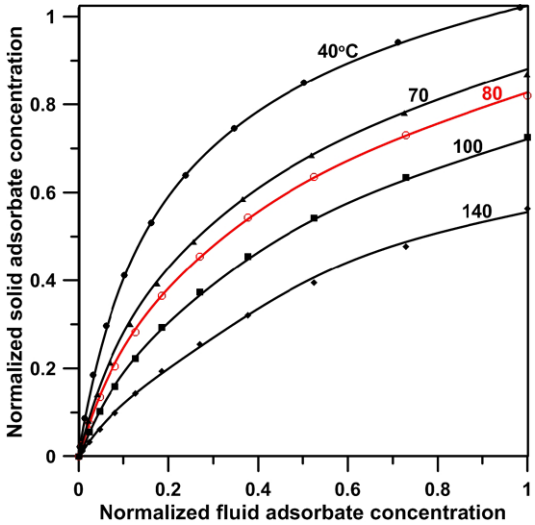

Fig. 7 FFNN for temperature-dependent TD Toth isotherm data sets. *Symbols* represent isotherm data set at different temperatures and *curves* represent FFNN fits. Data sets for 40, 70, 100 and 140 °C were used for training the neural network whereas the data set at 80 °C is used for validation

data set but a weaker predictive ability of the neural network for the validation data set was observed, thereby indicating that overfit prevailed.

5 Conclusion

In this study, the ability of neural networks was examined for their effectiveness to represent a wide array of adsorption isotherm data. It was found that the proposed models were highly effective to represent adsorption isotherms at a constant temperature with the flexibility to accurately fit data from all recognized (IUPAC) isotherm types. The extension of the neural network structure to incorporate temperature effects also proved to be excellent. The model proved adept at fitting isotherms of adsorbate-adsorbent systems over a wide range of temperature.

The power of the proposed neural isotherm models lies in the universality of its application. The ability of a single unifying model capable of representing data for all recognized types of adsorption isotherm models is an achievement that classic adsorption isotherm models cannot attain individually.

Acknowledgement The authors would like to acknowledge the Natural Science and Engineering Council of Canada (NSERC) for funding this project and for the scholarship awarded to Rudy Jones.

References

Basu, S., Henshaw, P.F., Biswas, N., Kwan, H.K.: Prediction of gas-phase adsorption isotherms using neural nets. Can. J. Chem. Eng. **80**, 1–7 (2002)

Bhat, N., McAvoy, T.: Use of neural nets for dynamic modeling and control of chemical process systems. In: American Control Conference, Pittsburgh, pp. 1336–1341 (1989)

Brunauer, S., Deming, L.S., Deming, W.E., Teller, E.: On a theory of the van der Waals adsorption of gases. J. Am. Chem. Soc. **62**, 1723–1732 (1940)

Bulsari, A.B., Palosaafi, A.: Application of neural networks for system identification of an adsorption column. Neural Comput. Appl. **1**, 160–165 (1993)

Carsky, M., Do, D.D.: Neural network modeling of adsorption of binary vapour mixtures. Adsorption **5**, 183–192 (1999)

Cybenko, G.: Approximation by superpositions of a sigmoidal function. Math. Control Syst. **2**, 303–314 (1989)

Freundlich, H.: Ueber die adsorption in loesungen. Z. Phys. Chem. **57**, 385–470 (1907)

Gao, W., Engell, S.: Neural-network based identification of nonlinear adsorption isotherms. In: IFAC Dynamics and Control of Process Systems, Cambridge, MA, USA, pp. 721–724 (2004)

Giraudet, S., Pré, P., Tezel, H., Le Cloirec, P.: Estimation of adsorption energies using physical characteristics of activated carbons and VOCs' molecular properties. Carbon **44**, 1873–1883 (2006)

Hoskins, J.C., Himmelblau, D.M.: Artificial neural network models of knowledge representation in chemical engineering. Comput. Chem. Eng. **12**(9/10), 881–890 (1988)

Kumar, K.V., Monteiro de Castro, M., Martinez-Escandell, M., Molina-Sabio, M., Rodriguez-Reinoso, F.: Neural network and principal component analysis for modeling of hydrogen adsorption isotherms on KOH activated pitch-based carbons containing different heteroatoms. Chem. Eng. J. **159**, 272–279 (2010)

Langmuir, I.: The Adsorption of Gases on plane surfaces of glass, mica and platinum. J. Am. Chem. Soc. **40**, 1361 (1918)

Lewandowski, J., Lemcoff, N.O., Palosaari, S.: Use of neural networks in the simulation and optimization of pressure swing adsorption processes. Chem. Eng. Technol. **21**(7), 593–597 (1998)

Mjalli, F., Al-Asheh, S., Banat, F., Al-Lagtah, F.: Representation of adsorption data for isopropanol-water system using neural network techniques. Chem. Eng. Technol. **28**(12), 1529–1539 (2005)

Padmesh, T.V.N., Vijayaraghavan, K., Sekaran, G., Velan, M.: Application of two-and three-parameter isotherm models: Biosorption of acid Red 88 onto Azolla microphylla. Bioremediation Journal **10**(1), 37–44 (2006)

Powell, M.J.D.: Some global convergence properties of a variable metric algorithm for minimization without exact line search. In: ASM/SIAM Symp. on Nonlinear Programming, New York (1975)

Sing, K.S.W., Everette, D.H., Haul, R.A.W., Moscou, L., Pierotti, R.A., Rouquérol, J., Siemieniewska, T.: Reporting physisorption data for gas/solid systems with special reference to the determination of surface area and porosity. Pure Appl. Chem. **57**, 603–619 (1985)

Sips, R.J.: On the structure of a catalyst surface. J. Chem. Phys. **16**, 490–495 (1948)

Sundaram, N.: Training neural networks for pressure swing adsorption processes. Ind. Eng. Chem. Res. **38**, 4449–4457 (1999)

Toth, J.: State equations of the solid gas interface layer. Acta Chem. Acad. Hung **69**, 311–317 (1971)

Vasina, E.N., Paszek, E., Nicolau, Jr., D.V., Nicolau, D.V.: The BAD project: data mining, database and prediction of protein adsorption on surfaces. Lab Chip **9**, 891–900 (2009)

Yang, M., Hubble, J., Fang, M., Locke, A.D., Rathbone, R.R.: A neural network for breakthrough prediction in packed bed adsorption. Biotech. Tech. **7**(2), 155–158 (1993)